www.amlett.com, www.vbripress.com/aml, DOI: 10.5185/amlett.2014.amwc474 Published online by the VBRI press in 2014

Iridium organic composite for organic light emitting devices for lighting

H. K. Dahule[1], S. J. Dhoble[2*]

[1]*Department of Physics, Shivaji Science College, Nagpur 440012, India*
[2]*Department of Physics, RTM Nagpur University, Nagpur 440033, India*

*Corresponding author. E-mail: sjdhoble@rediffmail.com

Received: 14 October 2013, Revised: 27 April 2014 and Accepted: 10 May 2014

ABSTRACT

We have synthesized series of new phosphorescent cyclometalated iridium (III) complexes $Ir(Br\text{-}DPQ)_2(acac)$, with 2-(4-bromo-phenyl)-4-phenyl-quinoline (Br-DPQ) ligand and $Ir(Cl\text{-}BrDPQ)_2$ (acac) with 4-chloro-2-(4-bromophenyl)-4-phenyl quinoline (Cl-BrDPQ) ligand. Synthesized complexes and ligands were characterized by X-ray diffraction, elemental analysis, infrared spectroscopy (FTIR) and thermal analysis (TGA/DTA,DSC). UV-vis absorption and emission spectroscopy, photoluminescence (PL) emission peaks of Br-DPQ and Cl-BrDPQ in different solvents such as chloroform, dichloromethane, THF, acetic acid and formic acid is between 425 to 460 nm The metal complex display pure red luminescence in solution and in powder states in the range of λmax 615-651 nm. The iridium metal complex $Ir(Br\text{-}DPQ)_2(acac)$ where (Br-DPQ=2-(4-bromo phenyl)-4-phenyl quinoline shows strong ^{1}MLCTand ^{3}MLCT absorption peak at, 227, 265, 283, 346, and 432 nm in tetrahydrofuran (THF) solution and $Ir(Cl\text{-}BrDPQ)_2(acac)$ where (Cl-BrDPQ)=4chloro2-(4-Bromo phenyl)-4-phenyl quinoline shows strong ^{1}MLCTand ^{3}MLCT absorption peak at 262, 330, 438, 476, 505 and 535 nm in dichloromethane solution. It is suggested that the synthesized iridium complexes may be efficiently used as the emissive dopants in phosphorescent organic light-lmitting devices (PhOLEDs). Thus these complexes could be promising candidates for potential applications in Phosphorescent organic light-emitting diodes PhOLEDs, light-emitting electrochemical cells and solid-state organic lighting applications. Copyright © 2014 VBRI press.

Keywords: Synthesis; photoluminescence; Iridium complex.

H. K. Dahule is an Associate Professor in the Department of Physics, Shivaji Science College, Congress Nagar Nagpur, India. He obtained his master's degree in Physics from R.T.M. Nagpur University, Maharashtra State, India. He pursued his doctorial thesis entitled 'Synthesis and Characterization of Iridium Based Complexes for Optoelectronic Devices' from RTM Nagpur University, Nagpur, India, in 2012. He received many awards and honors like best research paper presentation award and best research poster presentation award in various international/national conferences. He is Involved in research on Organic metal complexes for fabrication of OLED devices and Solar Cell.

S. J Dhoble obtained M.Sc. degree in Physics from Rani Durgavati University, Jabalpur, India in 1988. He obtained his Ph.D. degree in 1992 on Solid State Physics from Nagpur University, Nagpur. Dr. S. J. Dhoble is presently working as an Associate Professor in Department of Physics, R.T.M. Nagpur University, Nagpur, India. During his research carrier, he is involved in the synthesis and characterization of solid state lighting nanomaterials as well as development of radiation dosimetry phosphors using thermo-luminescence, mechano-luminescence and lyo-luminescence techniques. Dr. Dhoble published several research papers in International reviewed journals on solid-state lighting, LEDs, radiation dosimetry and laser materials. He is an executive member of Luminescence Society of India.

Introduction

Organic light emitting devices (OLEDs) is gaining large success in a new display technology **[1]**. A lot of efforts have been devoted for developing new materials in order to improve the efficiency of OLEDs. Cyclometalated iridium(III) complexes demonstrate high phosphorescent efficiencies and relatively short lifetimes among many different phosphorescent materials. Therefore, it is considered as one of the most promising phosphorescent dyes in OLEDs **[2, 3]** light-emitting electrochemical cells **[3]** biological labels **[4-5]** chemical sensors **[6, 7]** and solid-state organic lighting applications **[8]**. The attraction of these complexes comes from their higher chemical stability due to strong metal−ligand bonding interactions, as well as their longer excitation lifetimes and higher emission quantum yields **[9]**. Furthermore, the strong spin−orbit coupling induced by the central Ir(III) metal ion promotes an efficient intersystem crossing from the singlet to the triplet excited state manifold, which then facilitates strong electroluminescence by harnessing both singlet and triplet

excitons of the as fabricated optoelectronic devices **[10-12]**. As a result, syntheses of Ir(III) complexes have been extensively examined in the past two decades **[13-15]**. Since Baldo et al. **[4]** first reported high-efficiency green phosphorescent organic light-emitting diodes (OLEDs) based on fac-tris(2-phenylpyridine)iridium ($Ir(ppy)_3$), many efforts have been devoted to tailor the ligand structure in order to establish the relationship between structures of ligands and properties of the complexes, and then develop good materials for red **[5-8]**, green **[4, 9, 10]** and blue **[11-12]** OLEDs. It has been found that the emission wavelength of Ir (III) complexes can be tuned through choosing the appropriate subsitituents and changing their positions at 2-phenylpyridine ligand **[13]**, extending ligand conjugation and introducing strong donor–acceptor (DA) interaction in ligands **[5]**. So far, a number of cyclometalated ligands, including 2-arylisoquinoline **[5]**, which cans readily cyclometalate with iridium trichloride, have been investigated. Quinoline derivatives are nitrogen containing heterocyclic aromatic systems with advantages of ease of synthesis and purification. Although they have been used as ligands **[5, 14]** Ir (III) complexes containing quinoline ligands have not been studied systematically.

It is known that the HOMO of iridium(III) complexes is determined by the 5d orbital of Ir(III) with substantial mixing with the Π orbital of the ligand and the LUMO is related to the □* orbital of the ligand **[15]**. Thus, one can modulate HOMO and LUMO values of Ir(III) complexes to tune the emission color by changing the structure of the ligands.

The luminescence research field where in diverse application areas exist such as phosphor for high performance lamps, germicidal lamps which is used for the information display devices such as plasma TV, TFT monitor, CRT TV, OLED display used in mobile handset, photoluminescent liquid crystal display etc, light emitting diode. In the present work our concentration to developed new organic composite for OLED application

In this paper, we have synthesized new ligands with bromine and Clorine-Bromine substituents at para-position of 2-phenyl ring in 2, 4-diphenyl-quinoline (DPQ) unit. Corresponding bis-cyclometalated a orange red phosphorescent Ir(III) composite based on 2-(4-Bromo-phenyl)-4-phenyl-quinoline (Br-DPQ) and 4chloro 2-(4-Bromophenyl)-4-phenyl quinoline (Cl-BrDPQ) ligands were designed and synthesized and and their electrochemical, photo physical and electro phosphorescent properties were studied.

Experimental

All reagents and solvents were used as received without further purification. All reactions were performed under argon atmosphere.

Synthesis of ligand 2-(4-bromophenyl)-4 phenyl quinoline (Br-DPQ)

The quinoline-derived ligand 2-(4-Bromophenyl)-4 Phenyl quinoline (Br-DPQ)], were synthesized conveniently according to **Scheme 1** from the condensation of 2aminobenzophenone and 4-Bromo, acetophenone using the acid-catalyzed Friedlander reaction **[17]**.

2-Amino-benzophenone (2gm) $C_{13}H_{11}NO$ and Bromo acetophenone (2gm) were added along with Di-phenyl Phosphate (DPP) (2 gm), $C_{12}H_{11}O_4P$, and m-Cresol (3 ml) in a glass reactor fitted with mechanical stirrer, two glass inlets and one side arm. The reaction mixture was purged with argon for 20 min. and then the temperature was raised to 90 °C gradually under Argon atmosphere (99% pure) for 1 hour and then finally to 140 °C for 4 hours. After cooling, dichloromethane CH_2Cl_2, (50 ml) and 10 % NaOH (50 ml) were added to the reaction mixture. The organic layer was separated and washed with distilled water (20 ml x 5) until it was neutral, then dried over $MgSO_4$ and evaporated under vacuum to yield an off- white solid with some radish liquid on the top. The crude product was filtered and washed with hexane (5 ml x 3) to obtain crystalline solid of Bromo- Diphenylquinoline abbreviated as Br-DPQ.

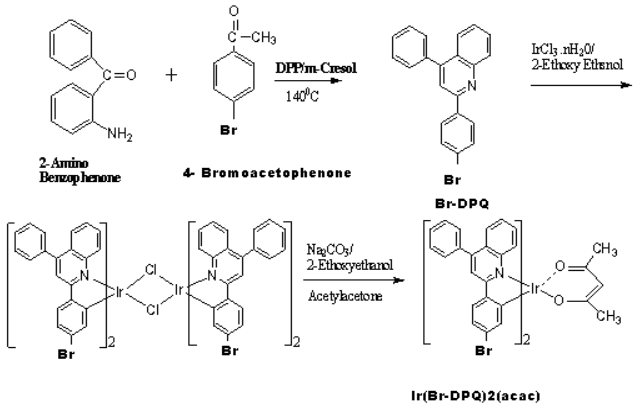

Scheme 1. Synthesis of Br-DPQ and $Ir(Br\text{-}DPQ)_2(acac)$.

Synthesis of ligand 6-chloro-2-(4-bromophenyl)-4 phenyl quinoline (Cl-Br-DPQ)

The quinoline-derived ligand 6-Chloro-2-(4-Bromophenyl)-4 Phenyl quinoline (Cl-Br-DPQ)], were synthesized conveniently according to Scheme 2 from the condensation of 2aminobenzophenone and 4-Bromo, acetophenone using the acid-catalyzed Friedlander reaction **[17]**. 2-Amino, 5-Chlorobenzophenone (2gm), and 4-Bromoacetophenone (2gm), were added along with Di-phenyl Phosphate (DPP) (2 gm), and m-Cresol (3 ml), in a glass reactor fitted with mechanical stirrer, two glass inlets and one side arm.

The reaction mixture was purged with argon for 20 min. and then the temperature was raised to 90 °C gradually under Argon atmosphere (99% pure) for 1 hour and subsequently to 140 °C for 4 hours. After cooling, dichloromethane– CH_2Cl_2, (50 ml) and 10 % NaOH (50 ml) were added to the reaction mixture.

The organic layer was separated and washed with distilled water (20 ml x 5) until it was neutral, then dried over $MgSO_4$ and evaporated under vacuum to yield an off-white solid with some radish liquid on top. The crude product was filtered and washed with hexane (5 ml x 3) to obtain crystalline solid of 6-Chloro-2-(4-Bromophenyl)-4Phenylquinoline.Chlorine–Bromine Diphenyl quinoline abbreviated as Cl-Br-DPQ.

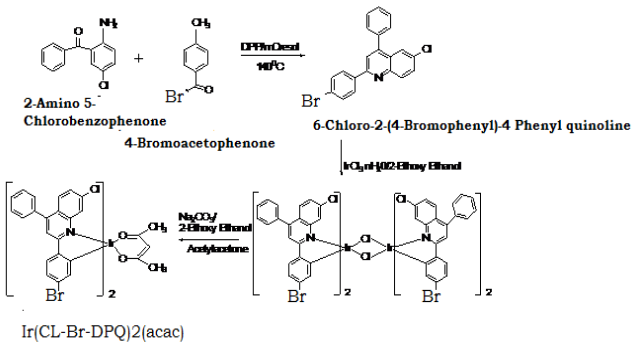

Scheme 2. Synthesis of Cl-Br-DPQ and Ir(Cl-Br-DPQ)$_2$(acac).

Synthesis of Ir(Br-DPQ)$_2$ (acac) complex

Cyclometalated Ir(III)-chloro-bridged dimers were synthesized according to the Nonoyama method **[18]**. Ir(Br-DPQ)$_2$ (acac) were synthesized according to **scheme 1**. Br-DPQ (2.2mmol) was dissolved in 2-methoxyethanol (10ml) in a 50ml round bottom flask. Iridium trichloride hydrate [$IrCl_3.3H_2O$] (1 m mol) and 3ml of water were then added into the flask. The mixture was stirred under argon atmosphere at 120 °C for 24 hrs. The mixture was cooled to room temperature and the precipitate was collected and then dried to give a cyclometallated chloride bridged dimmer as red powder. In a 50 ml flask, the cyclometallated chloride bridged dimmer, acetyl acetone (1.0 m mol) and Na_2CO_3 (2.5 m mol) were dissolved in 2ethoxyetenol (15 ml) and the mixture was the refluxed under an argon atmosphere for 12 hrs. After cooling to room temperature, the precipitate was filtered off and washed with water, ethanol and ether to give the desired product Ir(Br-DPQ)$_2$(acac) Yield 74.84 %.

Synthesis of Ir(Cl-Br-DPQ)$_2$ (acac) complex

Ir(Cl-BrDPQ)$_2$ (acac) were synthesized according to **Scheme 2**. Cl-Br-DPQ (2.2mmol) was dissolved in 2-methoxyethanol (10ml) in a 50ml round bottom flask. Iridium trichloride hydrate [$IrCl_3.3H_2O$] (1 m mol) and 3ml of water were then added into the flask. The mixture was stirred under argon atmosphere at 120 ^{O}C for 24 hrs. The mixture was cooled to room temperature and the precipitate was collected and then dried to give a cyclometallated chloride bridged dimmer as red powder. In a 50 ml flask, the cyclometallated chloride bridged dimmer, acetyl acetone (1.0 m mol) and Na_2CO_3 (2.5 m mol) were dissolved in 2ethoxyetenol (15 ml) and the mixture was the refluxed under an argon atmosphere for 12 hrs. After cooling to room temperature, the precipitate was filtered off and washed with water, ethanol and ether to give the desired product Ir(Cl-BrDPQ)$_2$(acac) Yield 75.04 %.

Measurements

A SHIMADZU 8101 FTIR spectrometer was used to record (IR) spectra. ^{1}H-nuclear magnetic resonance (NMR) and ^{13}C-NMR spectra were recorded using 300 MHz NMR Bruker spectrometers. Thermo gravimetric analysis TGA and SDTA was performed using Mettler STARe Thermo Gravimetric Analyzer, TGA/sDTA851e. Differential scanning calorimeter (DSC) analysis was carried out under nitrogen environment using Mettler Tolledo System. The XRD pattern was obtained by X-ray Panalytical diffractometer with Cu Kά radiation (λ=1.5418 Å) operated at 40 kV and 20 mA .The optical absorption spectra of complex and ligand in basic and acidic media in different molecular concentration were obtained on an Analytik Specord-50 spectrophotometer. The photoluminescence (PL) spectra were obtained by SHIMADZU RF 5301 spectrofluorometer

Results and discussion

XRD analysis

The crystallinity of the polyquinolines was evaluated by the wide-angle X-ray diffraction (XRD) experiments. X-ray diffraction analysis on powders of Br-DPQ, Cl-BrDPQ, Ir(Br-DPQ)$_2$(acac) and Ir(Cl-BrDPQ)$_2$ (acac) show many strong sharp diffraction peaks, as displayed in **Fig. 1** and **Fig. 2** respectively. Results reveal the polycrystalline character of the synthesized polymeric complexes. The weaker diffraction peaks indicate lower crystallinity or orientation. The crystallinity region contributes to sharp narrow diffraction peaks, while the amorphous component gives a very broad peak in the XRD data. Our results are similar to the earlier reported XRD results of Ir(ppy)$_3$ and Ir(btp)$_3$ powder samples. In organic devices, more commonly organic materials deposited either using the spin coating or evaporation processes form planar amorphous films.

FTIR analysis

In present work, the molecular Structure of Br-DPQ and Ir(Br-DPQ)$_2$(acac) was confirmed by FTIR spectra. The FTIR spectra were recorded on BRUKER model. The FTIR spectra of Br-DPQ, Ir(Br-DPQ)$_2$(acac) and Ir(Cl-BrDPQ)$_2$(acac) obtained from above model is shown in **Fig. 4**, in **Fig. 5** and in **Fig. 6**. The FTIR spectrum of Br-DPQ and Ir(Br-DPQ)$_2$(acac) has been taken by ATR method. The molecular confirmations of ligands and complex are done by FTIR spectra. The following FTIR peaks are obtained for the ligands and complex.

The characteristic peaks of FT-IR spectra of Br-DPQ are at 3745 , 3612, 3362, 2974, 2959, 2784, 1696, 1586, 1537, 1481, 1441, 1411, 1349, 1260, 1103, 1067, 1005, 827, 808 and 756 Cm $^{-1}$.

The characteristic peaks of FT-IR spectra of Ir(Br-DPQ)$_2$(acac) are at 3858, 3738, 3666, 3586, 3392, 3361, 2380, 2313, 2114, 1638, 1549, 1408, 1017, 930, 892, 842747 Cm $^{-1}$.

The characteristic peaks of FT-IR spectra of Ir(CL-Br-DPQ)$_2$(acac) are at 3737, 3738, 3015, 2913, 2314, 1582, 1531, 1474, 1441, 1345, 1213, 1144, 1062, 1019, 966, 877, 830, 806, 768, 693 Cm $^{-1}$.

Analysis of FTIR spectra of Ir(Br-DPQ)$_2$(acac) and Br-DPQ

The sharp variation occurs in the range 3600 – 3950 cm^{-1}[1], it may be due to single bond O-H stretching vibrations. The variations occur in the range 2800-3100 cm^{-1} was due to single bond C-H stretching vibrations. Generally, such variation's occurs in chelate compounds. Sharp and strong

absorbance was seen below 1625 cm^{-1}. This is because of carbonyl conjugated with the aromatic ring. The 1600-1500 cm^{-1} bands for the aromatic nucleus are variable (C=C Stretching vibrations). Four sharp absorbance peaks were observed in the spectra at 1625, 1600, 1550 & 1517 cm^{-1} in the region of double bond.

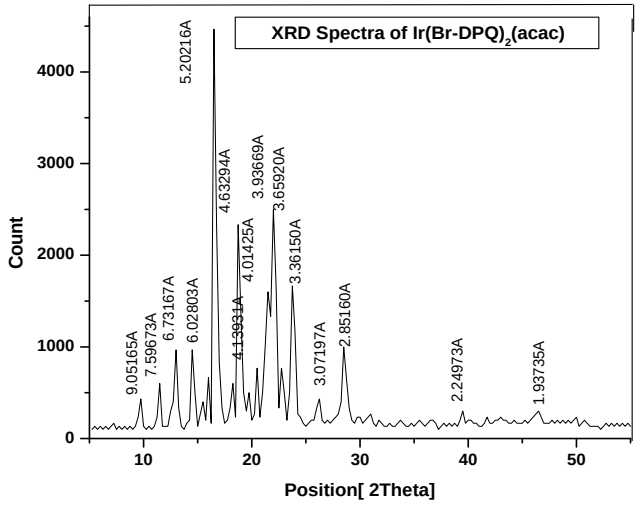

Fig. 1. XRD spectra of Ir(Br-DPQ)$_2$(acac).

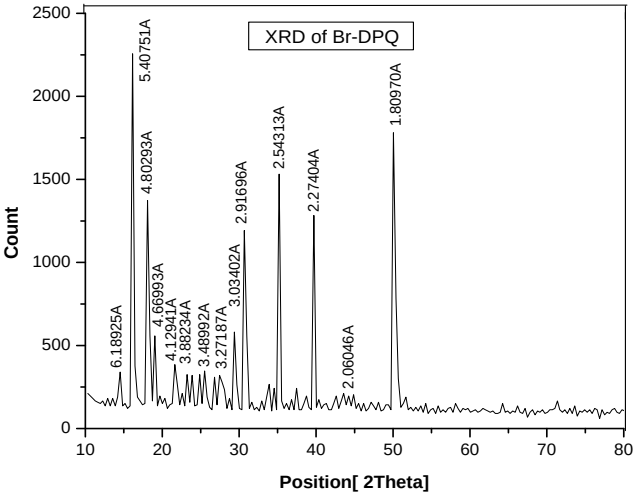

Fig. 2. XRD spectra of (Br-DPQ).

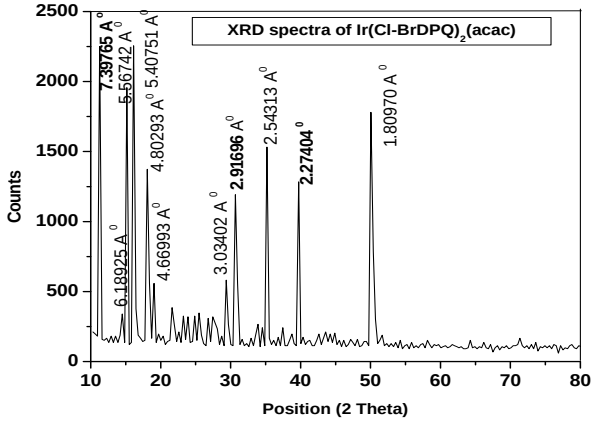

Fig. 3. XRD spectra of Ir(Cl-BrDPQ)$_2$(acac).

In a Finger print region (1500 – 600) large absorbance peaks were observed in the spectra due to CH bending vibrations. The peaks at 1025 & 1084 cm^{-1} may be due to C-O-C stretching vibrations. Maximum absorbance (80 %) was seen in the finger print region at 1262 cm^{-1}. The product was obtained from 4-Methoxy acetophenone, therefore it shows a strong peak due to asymmetric stretching for C-O-C of the ester. Other bands in this region may be related to the complex nature of the molecule. The peaks at 700, 788, 834 & 900 cm^{-1} may be due to CH out of plane bending vibrations in substituted ethylenic systems.

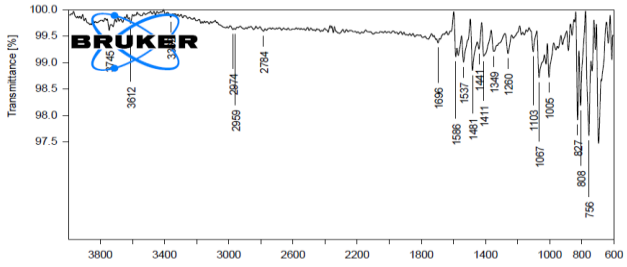

Fig. 4. The FTIR spectra of Br-DPQ.

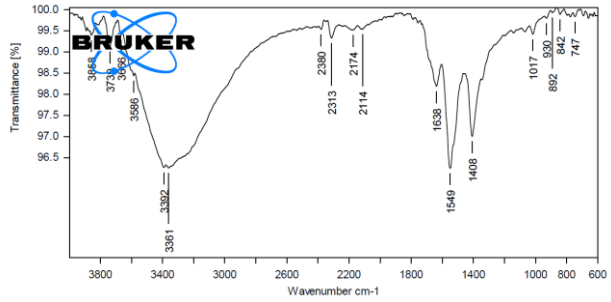

Fig. 5. The FTIR spectra of Ir(Br-DPQ)$_2$(acac).

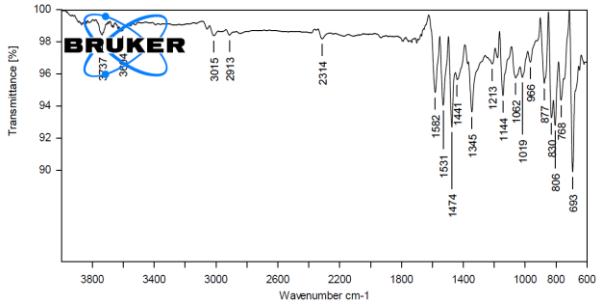

Fig. 6. The FTIR spectra of Ir(CL-Br-DPQ)$_2$(acac)

The peaks at 1084 and 1025 cm^{-1} are due to C-OH stretching vibrations secondary cyclic alcohols. The peaks at 1367, 1463 & 1488 cm^{-1} was due CH_2, CH_3 (CH) bending vibrations. Peaks at 1125, 1167, 1262 and 1288 cm^{-1} may be due to C-0-C vibrations. DPQ prepared by our group shows 76 % absorption at 1262 cm^{-1} and Cl-MO-DPQ shows 80 % absorption at same wave number.

Thermogravimetric analysis

The thermal properties of Br-DPQ and Ir(Br-DPQ)$_2$(acac) complexes were investigated by differential scanning calorimetry (DSC) measurement. DSC second heating scans of the polymeric compounds are shown in **Fig. 7**. Results indicate that Br-DPQ undergoes a glass transition at 42 °C, following by the crystallization at 105 °C and finally

the crystalline melting point at 304 °C (**Fig. 7**, curve a). In contrast, no such phase transition signal was observed in Ir(Br-DPQ)$_2$(acac) complex in the temperature range from 30 to 300 °C (**Fig. 7**, curve b).

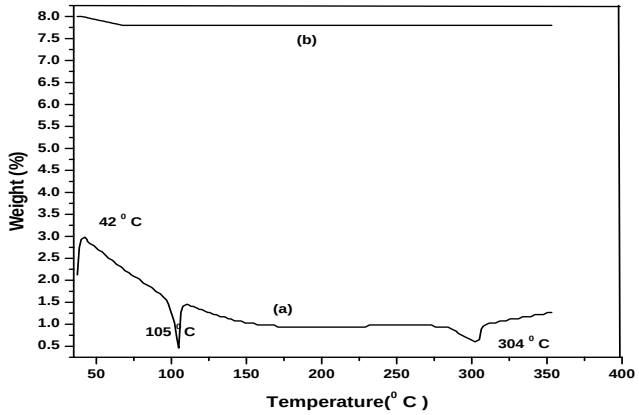

Fig. 7. DSC of Br-DPQ and Ir(Br-DPQ)$_2$(acac).

Furthermore, thermal stability, chemical reactivity and phase transitions properties of materials are evaluated by thermo gravimetric analysis (TGA) and differential gravimetric analysis (DTA). TGA is used for the precise measurement of the specimen weight changes as a function of time and temperature in various gaseous environments. DTA is used for measuring the changes in the specimen heat content during solid-state transformations and gas–solid reactions. The dynamic (non isothermal) DTA of Br-DPQ was performed in air atmosphere with a heating rate of 4 °C /min in a platinum crucible. **Fig. 8** shows TGA and SDTA curves of the Br-DPQ complex. The TGA curve displays three steps: a] No weight loss was observed in the first step of temperature range from 38 °C to 135 °C. i.e. there is no effect of temperature on a sample weight up to 135 °C. b). A small weight loss of about 0.794 % was observed in the second step of temperature range from 135 °C to 210 °C. The weight of the sample reduces to 12.4300 mg c) The total weight loss of about 1.59 % was observed in the third step of temperature range from 210 °C to 240 °C. In this step, the sample weight becomes 12.331 mg.

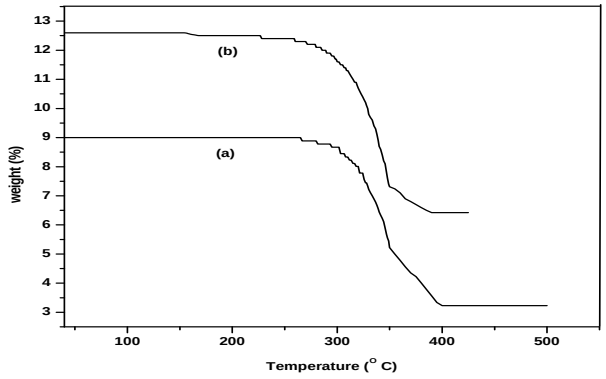

Fig. 8. TGA curve. (a) Ir(Br-DPQ)$_2$(acac) (b) Br-DPQ.

The TGA result of Br-DPQ complex, as seen in **Fig. 8**, supports the thermal stability of material over a wide range of temperature (220 °C), which is an imperative aspect for the operational devices. Similar results were observed in the Ir(Br-DPQ)$_2$(acac) complex. As compounds used in OLED fabrication are exposed to high temperature under the vacuum thermal evaporation condition, they should be stable over a temperature range of 200–350 °C The 5% weight reduction temperature in well known red phosphorescent emitters Ir(acac)$_3$ and Ir(piq)$_3$ are reported at 243 and 429 °C, respectively **[12]**, while the 10% weight loss temperature in Ir(btp)$_2$(acac) was at 368 °C.

Thermo gravimetric Analysis of Cl-BrDPQ and Ir(Cl-Br-DPQ)$_2$(acac)

Thermo gravimetric analysis plots of the Cl-Br-DPQ, obtained under the atmosphere of nitrogen, are shown in **Fig. 9**. The 10 % mass loss temperatures for the Cl-Br-DPQ were found to be 327 °C. This result indicates that incorporation of the Cl substitution improves the thermal stability of the DPQ matrix. The different types of dopants have different influence on the thermal stability of DPQ matrix. Based on the comparison of the obtained results with above-mentioned literature data we can conclude that in the presence of the Cl thermal stability of the DPQ is moderately improved.

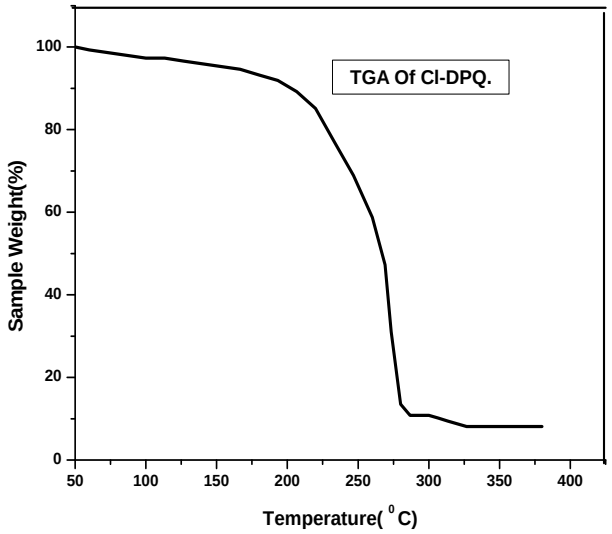

Fig. 9. TGA curve of Cl-Br-DPQ.

Thermo gravimetric analysis of the Ir(Cl-Br-DPQ)$_2$(acac) is shown in **Fig. 10**. From **Fig 10** it is clear that the complex is thermally stable up to 350 °C. A weight loss (2.0444 %) at 375 °C might be attributed to the loss of some absorbed water molecules. In the second step weight loss of about 8.444 % were taken place up to 400 °C. The weight loss start at 350 °C and completed at 450 °C. This huge weight loss suggests that the decomposition of complex start in this range, hence complex was stable up to this temperature.

We investigated the thermal properties of Ir(Cl-Br-DPQ)$_2$(acac) and Cl-Br-DPQ by differential scanning calorimetry (DSC). The DSC second heating scans of the polymeric compound are shown in **Fig. 11** (curve (a) and Curve (b)).

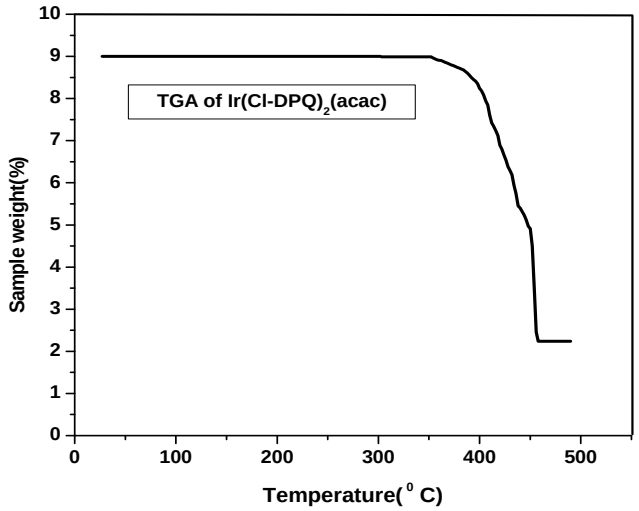

Fig. 10. Thermo gravimetric analysis curve of Ir(Cl-DPQ)$_2$(acac).

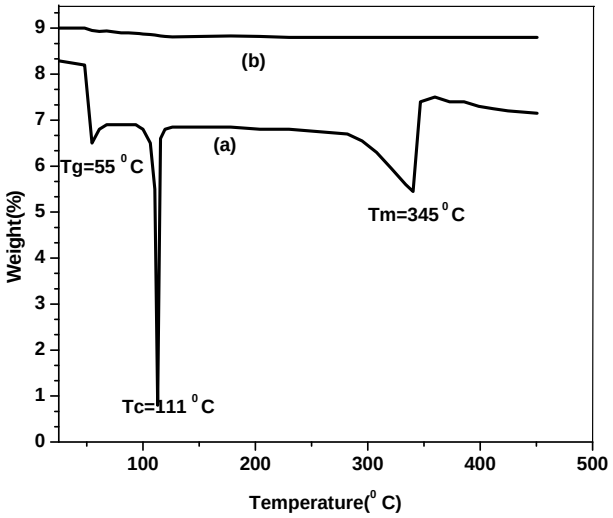

Fig. 11: DSC scan of (a) Cl- Br DPQ.(b)Ir(Cl-BrDPQ)$_2$(acac).

In **Fig. 11** curve (a) indicate that Cl-DPQ undergoes a glass transition at 55 °C, following by crystallization at 111 °C and crystalline melting point at 345 °C. In contrast, there was no phase transition signal observed for Ir(Cl-DPQ)$_2$(acac) from 30 to 450 °C as shown in **Fig. 11** curve (b).

The DSC cooling curves of the Cl-BrDPQ and Ir(Cl-Br-DPQ)$_2$(acac) is shown in **Fig. 11** for the temperature range from 10 to 500 °C . In the lower temperature region DSC measurements indicated that incorporation of the Cl induces change of the melting transition temperature of the DPQ. The change of the glass transition temperature can be considered as a measure of polymeric compound immobilization. Because the Cl is chemically bound to the DPQ chains, they are capable to induce the increase of the glass transition temperature. The decomposition temperature is found to be 345 °C.

Photophysical properties

UV–vis absorption spectra of 10^{-4} M solutions of Br-DPQ complex in Chloroform, DCM and THF Solution at room temperature are shown in **Fig. 12**. The compound Br-DPQ shows broad absorption band ranging from 240 to 390 nm with a λ_{max} at around 272 nm and a shoulder at 327 nm in DCM and peak at 269 and 332 nm in Chloroform and THF solutions. The PL emission of Br-DPQ in powder form is shown in **Fig. 12**.

The excitation spectra of Br-DPQ crystalline powder exhibits a peak at 255 nm (result not reproduced here). When the powder is excited at 255 nm, intense light emission appears at the wavelength of 450 nm.

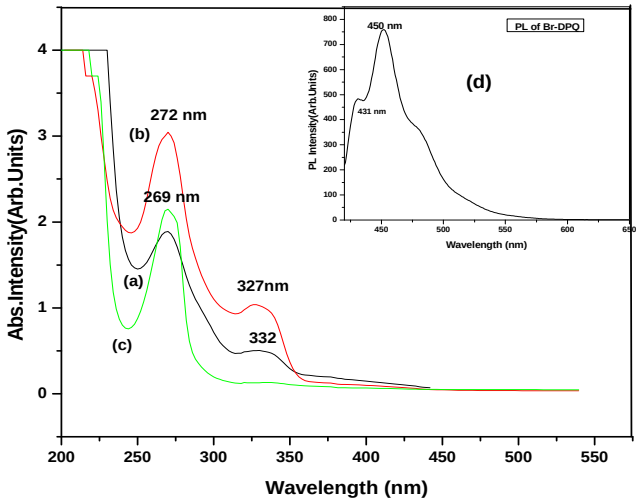

Fig. 12. Absorbance spectra of Br-DPQ in (a)Chloroform, (**b**) DCM & (c) THF Solution (d) PL spectra of Br-DPQ in THF Solution.

The absorption and photoluminescence emission spectra measured for 10^{-4}M solutions of Ir(Br-DPQ)$_2$(acac) in DCM, THF and formic acid at room temperature are displayed in **Fig. 13**. The strong absorption bands in the UV region are assigned to the spin-allowed 1π–π* transition of the cyclometalated quinoline ligands. The lowest energy absorption peak in the region 440–460 nm could be ascribed to a typical spinallowed metal-to-ligand charge transfer (1MLCT) transition. We believe the weak bands at the long wavelength side are associated to both spin–orbit coupling enhanced 3π–π* and ^{3}MLCT transitions. It is noted that the formally spin forbidden ^{3}MLCT transition gains intensity by mixing with the higher-lying 1MLCT transition through the strong spin–orbit coupling of Ir, which is comparable to the allowed 1MLCT transition. Furthermore, we have observed absorption peaks at 227, 265, 283, 346, and 432 nm in THF. The highly intense PL emission peak of Ir(Br-DPQ)$_2$(acac) complex in THF was located in the red region with the λmax value at 615 nm in THF CIE coordinates of (0.676, 0.316). However the emission peaks of the complex Ir(Br-DPQ)$_2$(acac) in different solvents show clear differences. This emission of complex Ir(Br-DPQ)$_2$(acac) peaks at around 616 nm in solid state ,620 in THF (polar solvent) and 624 nm in CH_2Cl_2 (medium polarity) and 628 nm in acetic acid. The peak shift can be attributed to the stronger interaction (are shown in **Fig. 14**) between the solvents and the excited molecules. The broad, structure less spectral features lead us to conclude that the phosphorescence originates primarily from the ^{3}MLCT state.

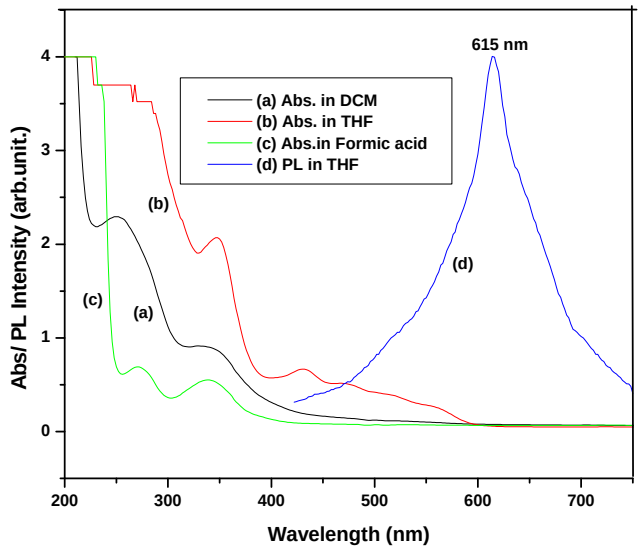

Fig. 13. Absorbance spectra of 10^{-4} M solutions of Ir(Br-DPQ)$_2$(acac) in (**a**)DCM, (**b**) THF & (**c**) Formic acid Solution (**d**) PL spectra of Ir(Br-DPQ)$_2$(acac) in THF Solution.

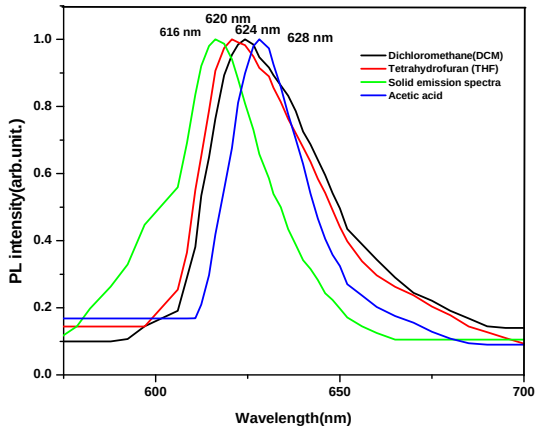

Fig. 14. .PL spectra of Ir(Br-DPQ)$_2$(acac).

Photo physical properties of Cl-Br-DPQ and Ir(Cl-Br-DPQ)$_2$(acac) complex

The optical properties of ligand Cl-Br-DPQ and Ir(Cl-Br-DPQ)$_2$(acac) complex were measured in basic solvents i.e. chloroform, dichloromethane solutions and in acids i.e. acetic acid and formic acid. The compound Cl-Br-DPQ shows broad absorption band ranging from 240 to 390 nm with a λ_{max} at around 273 nm and a shoulder at 341 nm in both solutions. Photoluminescence (PL) emission peaks in different solvents such as chloroform, dichloromethane, acetic acid and formic acid are between 421 to 446nm. We observed highly intense photoluminescence (PL) are shown in **Fig. 15**, for Ir(Cl-Br-DPQ)$_2$(acac) in THF with values of λmax located at 651 nm with CIE coordinates of (0.715,0.283). The broad, structure less spectral features lead us to conclude that the phosphorescence originates primarily from the ^{3}MLCT state, are shown in **Fig. 16**.

Electroluminescence of organic materials

In present work, we have prepared EL-cells of Br-DPQ to study electroluminescence properties. In present investigations, we have restricted our study to EL-measurements: brightness versus voltage and current versus voltage.

Brightness-voltage characteristics curve for Br-DPQ

The **Fig. 17** shows brightness-voltage characteristics curve for Br-DPQ cell. It was found that electroluminescence begins at 400V and then after brightness increases exponentially with applied AC voltage. This means it exhibits same characteristics as earlier EL cell.

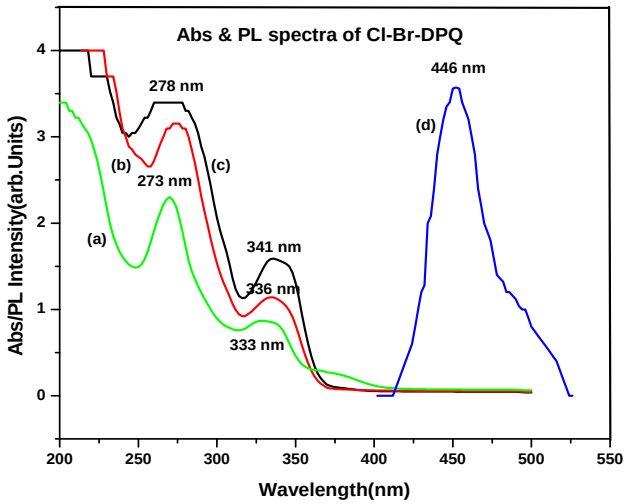

Fig.15. Abs and PL spectra of ligand.

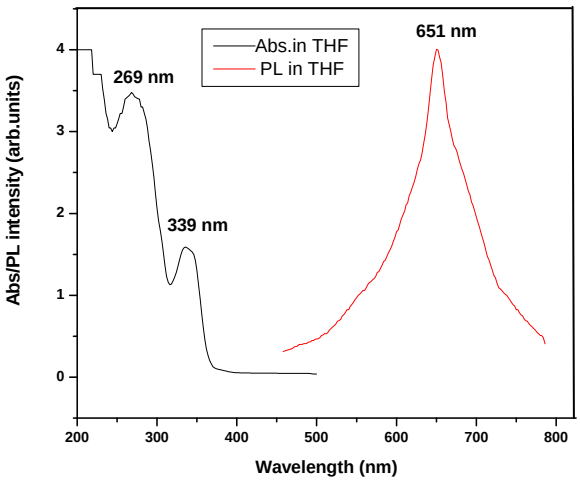

Fig. 16. Abs and PL spectra of Ir(Cl-BrDPQ)$_2$(acac) complex.

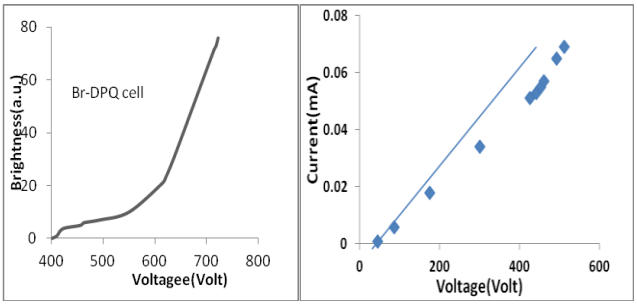

Fig. 17. Brightness-voltage characteristics for Br-DPQ cell.

The linear relation has been observed between current and voltage for Br-DPQ sample which represents ohmic nature, as shown in **Fig. 17**. Such ohmic behavior can be attributed to hoping conductivity of electrons through a fine emissive layer. It was observed that this sample emits blue color under electric field.

Conclusion

We have successfully synthesized a new red emitting Ir(III) phosphorescent complexes Ir(Br-DPQ)$_2$(acac) and Ir(Cl-BrDPQ)$_2$(acac) bearing a 2-(4-Bromo phenyl)-4 Phenyl quinoline (Br-DPQ) and 6-Chloro-2-(4-Bromophenyl)-4. Phenyl quinoline (Cl-Br-DPQ)] Ligand respectively. The synthesized complex is thermally very stable over a wide range of temperature and suitable for the use as a red-emissive material in OLEDs.

Reference

1. Ho, C.L.; Wong, W.Y.; Zhou,G.J.; Yao, B.; Xie, Z.; Wang, L.; *Adv. Funct. Mater.* **2007**, *17*, 2925. **DOI:** 10.1002/adfm.200601205
2. Kang, D.M.; Kang, J.W.; Park, J.W.; Jung, S.O.; Lee, S.H; Park, H.D.; Kim, Y.H.; Shin, S.C.; Kim, J.-J.; Kwon, S.K.; *Adv. Mater.* **2008**, *20*, 2003. **DOI:** 10.1002/adma.200702558
3. Lowry, M. S.; Bernhard, S.; Chem. *Eur. J.* **2006**, *12*, 7970. **DOI:** 10.1002/chem.200600618
4. Peng, Y.K.; Lai, C.W.; Liu, C.L.; Chen, H.C.; Hsiao, Y.H.; Liu, W.L.; Tang, K.C.; Chi, Y.; Hsiao, J.K.; Lim, K.E.; Liao, H.E.; Shyue, J.J.; Chou, P.T.; *ACS Nano* **2011**, 5, 4177. **DOI:** 10.1021/nn200928r
5. You, Y.; Lee, S.; Kim, T.; Ohkubo, K.; Chae, W.S.; Fukuzumi, S.; Jhon, G.J.; Nam, W.; Lippard, S. J.; *J. Am. Chem. Soc.* **2011**, *133*, 18328. **DOI:** 10.1021/ja207163r
6. Zhang, K. Y.; Li, S. P.Y.; Zhu, N.; Or, I.W.S.; Cheung, M.S.H.; Lam, Y.W.; Lo, K.K.; *Inorg. Chem.* **2010**, *49*, 2349. **DOI:** 10.1021/ic902225f
7. Ho, M.L.; Hwang, F.M.; Chen, P.N.; Hu, Y.H.; Cheng, Y.M.; Chen, K.S.; Lee, G.H.; Chi, Y.; Chou, P.T.; *Org. Biomol. Chem.* **2006**, *4*, 98. **DOI:** 10.1039/B511943J
8. Dahule, H.K.; Dhoble, S.J.; Ahn, J.S.; Pode R.B.; *J. Phys. Chem. Solids* **2011**, *72*, 1524. **DOI:** pii/S0022369711002885
9. Kamtekar, K.T.; Monkman, A.P.; Bryce, M.R.; *Adv. Mater.* **2010**, *22*, 572. **DOI:** 10.1016/j.jpcs.2011.09.011
10. Thompson, M.E.; *MRS Bull.* **2007**, *32*, 694 **DOI:** 10.1557/mrs2007.144
11. Rausch, A.F.; Homeier, H.H.H.; Yersin, H.; *Top. Organomet. Chem.* **2010**, *29*, 193. **DOI:** 10.1007/3418_2009_6
12. Chou, P.T.; Chi, Y.; Chung, M.W.; Lin, C.C.; *Coord. Chem. Rev.* **2011**, *255*, 2653. **DOI:** pii/S0010854510002638
13. Yersin, H.; Rausch, A.F.; Czerwieniec, R.; Hofbeck, T.; Fischer, T.; *Coord. Chem. Rev.* **2011**, *255*, 2622. **DOI:** pii/S0010854511000403
14. Ulbricht, C.; Beyer, B.; Friebe, C.; Winter, A.; Schubert, U. S.; *Adv. Mater.* **2009**, *21*, 4418. **DOI:** 10.1002/adma.200803537
15. Chi, Y.; Chou, P.T.; *Chem. Soc. Rev.* **2010**, *39*, 638. **DOI:** 2010/cs/b916237b
16. Sasabe, H.; Kido, J.; *Chem. Mater.* **2011**, *23*, 621 **DOI:** 10.1021/cm1024052
17. Fehnel, E.A.; *J. Org. Chem.*, **1966,** *31*, 2899. **DOI:** 10.1021/jo01347a038
18. Nonoyama, M.; *Bull. Chem. Soc. Jpn*. **1974**, *47*, 767. **DOI:** 10.1246/bcsj.47.767

